Scattering by Thin Dielectric Strips

JACK H. RICHMOND, FELLOW, IEEE

Abstract—**A plane wave incident on a thin dielectric strip with infinite length is considered, letting the incident electric field vector be parallel with the edges of the strip. The field is expanded in the dielectric region as the sum of three plane waves (the forced wave and two surface waves). The x-axis and y-axis propagation constants are known for each wave, and Galerkin's method is employed to determine the amplitudes of these waves. Finally, the far-zone scattered field is determined by considering the polarization currents radiating in free space. Numerical data are presented to illustrate the scattering properties of lossless and lossy dielectric strips as a function of the angle of incidence and the width of the strip. The calculations show excellent agreement with an earlier moment method using pulse bases and point matching.**

I. INTRODUCTION

A DIELECTRIC strip with infinite length, width w, and thickness d is illustrated in Fig. 1. A plane wave is incident on this strip, and the incident electric field vector is parallel with the edges of the strip. This geometry is of interest in connection with certain antenna design problems.

This problem was treated by Richmond [1] in 1965 with the moment method, but the technique becomes inefficient as the width of the strip increases. Burnside and Burgener [2] presented the geometrical theory of diffraction (GTD) analysis, but they neglected the surface waves which propagate on the strip. Kastner and Mittra [3] presented the spectral-iteration technique, but they encountered difficulties as the width of the strip increased. Pathak and Rojas-Teran [4] obtained excellent results with the Wiener–Hopf procedure, except for difficulties in the vicinity of grazing incidence.

In this paper we expand the field in the dielectric strip as the sum of three plane waves: the forced wave and two surface waves. The form is known for each wave, but the amplitude is unknown. We apply Galerkin's technique to develop three equations for the three unknown amplitudes. Finally, the far-zone scattered field is determined by considering the electric polarization current radiating in free space.

We present the theory in the next section. This is followed by numerical results for the scattering levels of thin dielectric strips versus the angle of incidence and the width.

II. THEORY

Consider a time-harmonic wave incident on a thin dielectric strip, as illustrated in Fig. 2. The time dependence $e^{j\omega t}$ is assumed and suppressed. In this two-dimensional problem, we let the electric field intensity E have only a z-component which is independent of z. At each point in space,

$$E = E^i + E^s \tag{1}$$

where E, E^i, and E^s denote the total field, incident field, and

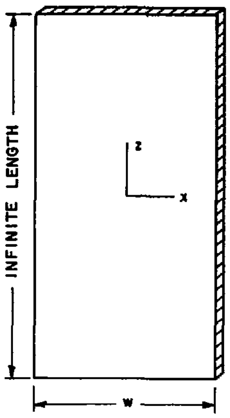

Fig. 1. Dielectric strip and coordinate system.

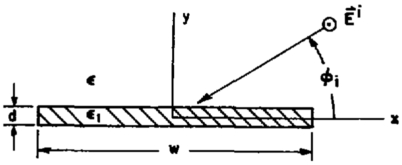

Fig. 2. Cross-sectional view of thin dielectric strip with incident plane wave.

scattered field, respectively. Since the electric field has only a z-component, this scalar notation is suitable.

The scattered field can be generated by the equivalent electric polarization-current density

$$J = j\omega(\epsilon_1 - \epsilon)E \tag{2}$$

radiating in the unbounded homogeneous ambient medium with parameters μ and ϵ. We consider the dielectric strip to be homogeneous, with permittivity ϵ_1 and permeability $\mu_1 = \mu$. (If μ_1 differed from μ, the scattered field would have another contribution from the magnetic polarization current.) We let ϵ_1 be complex to represent a lossy dielectric material. At each point in space, the scattered field is given by

$$E^s(x, y) = -(\omega\mu/4)\iint J(x', y')H_0(kR)\, dx'\, dy' \tag{3}$$

$$R^2 = (x' - x)^2 + (y' - y)^2 \tag{4}$$

$$k^2 = \omega^2\mu\epsilon. \tag{5}$$

In (3) the integration extends over the cross-sectional surface of the dielectric strip, and $H_0(kR)$ denotes the Hankel function of the second kind.

From (1), (2), and (3) we obtain the integral equation

$$E(x, y) + j(k^2/4)(\epsilon_r - 1)\iint E(x', y')H_0(kR)\, ds' = E^i(x, y) \tag{6}$$

where $\epsilon_r = \epsilon_1/\epsilon$ and $ds' = dx'dy'$. The integration extends over the cross-sectional surface of the dielectric strip.

Manuscript received June 4, 1984. This work was supported in part by the Joint Services Electronics Program under Contract N00014-78-C-0049 with The Ohio State University Research Foundation.

The author is with the ElectroScience Laboratory, Department of Electrical Engineering, The Ohio State University, Columbus, OH 43212.

0018-926X/85/0100-0064$01.00 © 1985 IEEE

In the moment method [5], the next step is to expand the unknown function $E(x, y)$ in a series of basis functions. We selected the following series for the field in the dielectric strip:

$$E(x,y) = \sum_{n=1}^{3} C_n \exp(f_n x) \cosh(g_n y) \tag{7}$$

$$f_n^2 + g_n^2 = -\omega^2 \mu \epsilon_1. \tag{8}$$

We choose the propagation constants f_n and g_n so that the wave $n = 1$ represents the forced wave, wave 2 is a surface wave propagating in the negative x direction, and wave 3 is a surface wave propagating in the positive x direction.

By "forced wave," we mean the field induced in an infinitely wide dielectric slab by an incident plane wave. Referring to Fig. 2, we see that the propagation constant of the forced wave is

$$f_1 = jk \cos \phi_i. \tag{9}$$

For the surface wave ($n = 2$), the propagation constant is determined from (8) and the transcendental equation

$$g_2 \tanh(g_2 t) = -\sqrt{-k^2 - f_2^2} \tag{10}$$

$$t = d/2. \tag{11}$$

The theory of the surface wave is presented in the Appendix. Since mode 3 is a surface wave propagating in the opposite direction, $f_3 = -f_2$.

For the surface wave on a thin dielectric slab, it turns out that E_z is an even function of y. For the forced mode, E_z has even and odd components but the even component dominates if the slab is thin and $\mu_1 = \mu$. For these reasons, we represent the field in the strip as an even function of y in (7).

The three modes in (7) form an incomplete set, and we may hope for success only if the true field in the dielectric strip is dominated by these three modes. If the dielectric strip were thick enough to support higher-order surface waves, one would have to include them in (7).

It may be helpful to compare our basis functions for the dielectric strip with the GTD modes on a perfectly conducting strip. The forced mode on the dielectric strip is analogous to the physical-optics current wave on the conducting strip. Furthermore, the surface waves on the dielectric strip are analogous to the creeping waves on the conducting strip. Thus, in our approach to the dielectric strip, we are using the moment method in combination with GTD basis functions.

From (6) and (7), we obtain the following equation which holds at each point within the dielectric strip:

$$\sum_{n=1}^{3} C_n \left[\exp(f_n x) \cosh(g_n y) + j(k^2/4)(\epsilon_r - 1) \iint \exp(f_n x') \cosh(g_n y') H_0(kR)\, ds' \right] = E^i(x,y). \tag{12}$$

In the moment method, the next step is to choose a set of testing or weighting functions $W_m(x, y)$. We selected the functions

$$W_m(x,y) = \exp(-f_m x) \cosh(g_m y), \qquad m = 1, 2, 3. \tag{13}$$

Except for a sign reversal in the exponent, these weighting functions are the same as the basis functions in (7). Each basis function represents a wave traveling across the dielectric strip, and the corresponding weighting function represents a wave traveling in the opposite direction across the strip. In Galerkin's method the weighting functions are the same as the basis functions or the complex conjugate of the basis functions. With the goal of obtaining an impedance matrix that is symmetric and diagonally dominant, we deviated slightly from Galerkin's method.

Multiplying both sides of (12) by $W_m(x, y)$ and integrating over the cross section of the strip, we obtain the following system of simultaneous linear equations:

$$\sum_{n=1}^{3} C_n Z_{mn} = V_m \qquad m = 1, 2, 3 \tag{14}$$

$$V_m = \iint \exp(-f_m x) \cosh(g_m y) E^i(x,y)\, ds \tag{15}$$

$$Z_{mn} = S_{mn} + T_{mn} \tag{16}$$

$$S_{mn} = j(k^2/4)(\epsilon_r - 1) \cdot \iiiint \cosh(g_m y) \cosh(g_n y') \cdot \exp(f_n x' - f_m x) H_0(kR)\, d_s'\, ds \tag{17}$$

$$T_{mn} = \iint \cosh(g_m y) \cosh(g_n y) \exp(f_n x - f_m x)\, ds. \tag{18}$$

It can be shown that the impedance matrix is symmetric, so that $Z_{mn} = Z_{nm}$. The incident plane-wave field is given by

$$E^i = E_0 \exp(jkx \cos \phi_i) \exp(jky \sin \phi_i). \tag{19}$$

In (15), the limits of integration are $x = \pm h$ and $y = \pm t$ where $h = w/2$. From (15) and (19), the excitation voltages are given by

$$V_m = E_0 X_m Y_m \tag{20}$$

$$X_m = w \operatorname{Sinh}[(f_1 - f_m)h] \tag{21}$$

$$Y_m = t[\operatorname{Sinh}[(g_0 + g_m)t] + \operatorname{Sinh}[(g_0 - g_m)t]] \tag{22}$$

$$h = w/2 \tag{23}$$

$$\operatorname{Sinh}(z) = \frac{\sinh(z)}{z} \tag{24}$$

where $g_0 = jk \sin \phi_i$ and $X_1 = w$.

The integrals in (18) are easy to evaluate, with the following result:

$$T_{mn} = X_{mn} Y_{mn} \tag{25}$$

$$X_{mn} = w \operatorname{Sinh}[(f_n - f_m)h] \tag{26}$$

$$Y_{mn} = t[\operatorname{Sinh}[(g_n + g_m)t] + \operatorname{Sinh}[(g_n - g_m)t]]. \tag{27}$$

In evaluating S_{mn} we use a change of variables (such as $v = x' - x$ and $s = y' - y$) to reduce the number of integrations required. The range of integration is split into three regions. When kR is small, we employ the small-argument form for the Hankel function. When kR is large, we use the large-argument form to express S_{mn} in terms of complex error functions. In the intermediate region, we employ numerical integration techniques.

The constants C_n are determined from (14), and the scattered field (from (2), (3), and (7)) is calculated as follows:

$$E^s(x,y) = -j(k^2/4)(\epsilon_r - 1) \sum_{n=1}^{3} C_n \iint \exp(f_n x') \cdot \cosh(g_n y') H_0(kR)\, ds'. \tag{28}$$

The far-zone scattered field is obtained from (28) and the large-argument form for the Hankel function [6], as follows:

$$E^s(\rho, \phi_s) = -j(k^2/4)(\epsilon_r - 1)\sqrt{\frac{2j}{\pi k\rho}}\; e^{-jk\rho} \sum_{n=1}^{3} C_n F_n(\phi_s) \tag{29}$$

$$F_n(\phi) = \iint \exp\,(f_n x + jkx \cos\phi) \exp\,(jky \sin\phi) \cdot \cosh\,(g_n y)\; dx\, dy \tag{30}$$

$$F_n(\phi) = X_n Y_n \tag{31}$$

$$X_n = w \operatorname{Sinh}\,[(f_n + f_0)h] \tag{32}$$

$$Y_n = t[\operatorname{Sinh}[(g_n + g_0)t] + \operatorname{Sinh}\,[(g_n - g_0)t]] \tag{33}$$

$$f_0 = jk \cos\phi \tag{34}$$

$$g_0 = jk \sin\phi. \tag{35}$$

III. NUMERICAL RESULTS

In this section we present some numerical results for a thin dielectric strip with thickness $d = 0.025\ \lambda_0$. The ambient medium is free space, and λ_0 denotes the wavelength in free space. The permittivity of the dielectric strip is $\epsilon_1 = 4\epsilon_0(1 - j \tan\delta)$. Data are included for lossless strips ($\tan\delta = 0$) and lossy strips with $\tan\delta = 0.1$. For a surface wave propagating on this strip, the electric field intensity in the dielectric region is $E = \exp(\pm fx)\cdot \cosh(gy)$. Letting $f = \alpha + j\beta$, we used the theory in the Appendix to determine that $\alpha = 0$ for the lossless strip and $\alpha = 0.0438$ Np/m for the lossy strip ($\tan\delta = 0.1$) at 300 MHz. Let c denote the velocity of light in free space, and let v denote the phase velocity of the surface wave. We found that $v/c = 0.9732$ and 0.9737 for the lossless and lossy strips, respectively. Now β and v are related as follows: $\beta = k_0 c/v$.

Fig. 3 illustrates the electric field distribution $E_z(x)$ induced in a thin dielectric strip by a plane wave with grazing incidence ($\phi_i = 0$). The incident field strength is 1 V/m. As shown in Fig. 2, x is measured from the center of the strip. As a check, we calculated the field distribution by two methods. In the old method (pulse bases), the dielectric strip was divided into 200 square cells and we generated a system of 200 simultaneous linear equations. In the new method (plane-wave expansion), the field in the dielectric strip was represented as the sum of three plane waves, and we generated a system of three simultaneous linear equations. It is evident in Fig. 3 that the two methods show good agreement. The amplitudes of the three plane waves are tabulated in Fig. 3.

Fig. 4 illustrates the backscatter pattern for the same dielectric strip that we considered in Fig. 3.

Fig. 5 illustrates forward scattering versus the width of the strip with grazing incidence. As the width increases, the pulse-basis technique requires ever increasing computational time and storage. When the width is equal to 25 wavelengths, there are 1000 unknowns and the central processing unit (CPU) time is 120 s on a VAX 11/780 computer. For this reason, the pulse-bases calculations were terminated at this point. Although the results are not shown in Fig. 5 for narrow strips, the calculations (with the plane-wave expansion and with the pulse bases) show excellent agreement for all widths from $w = 0$ to $w = 25\ \lambda_0$.

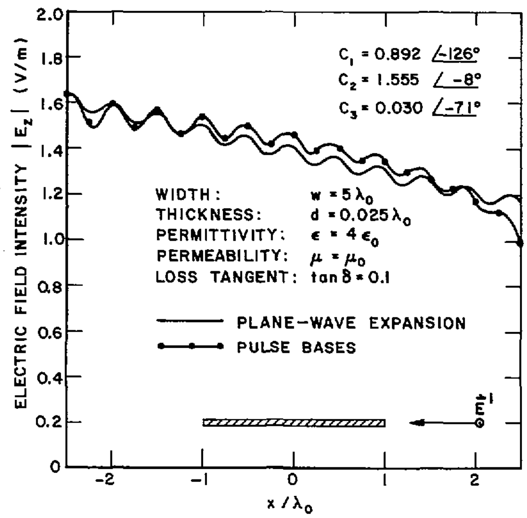

Fig. 3. Electric field distribution induced in thin dielectric strip by plane wave with grazing incidence.

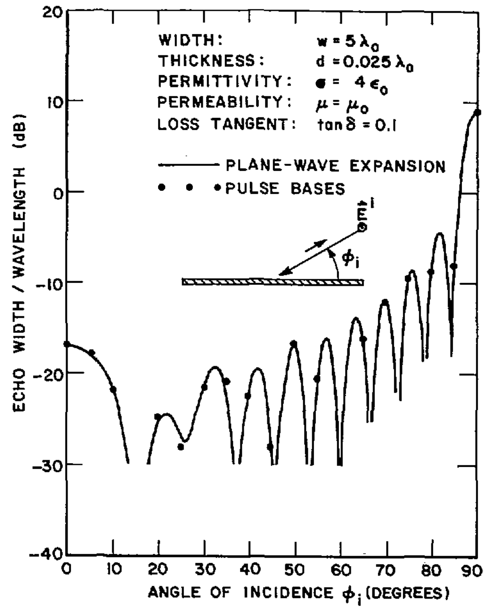

Fig. 4. Backscatter pattern for thin dielectric strip.

Fig. 6 illustrates backscatter versus width for dielectric strips with grazing incidence, as calculated with pulse bases. In Figs. 7 and 8, it may be noted that the new plane-wave expansion shows excellent agreement with pulse bases for lossless and lossy strips with grazing incidence.

All calculations were carried out on a VAX 11/780 computer. With the plane-wave expansion the computational time is approximately 0.3 s to solve for the backscatter or bistatic scatter from a lossless or lossy thin dielectric strip. For comparison, Fig. 9 illustrates the computational time with pulse bases when we take advantage of the Toeplitz nature of the impedance matrix.

The limitations of the new technique have not yet been established, but the method should not be relied on if the thickness d of the strip exceeds one skin depth or one tenth of the wavelength in the dielectric medium.

IV. SUMMARY AND CONCLUSION

In this report we consider a plane wave to be incident on a thin dielectric strip with infinite length, and the incident electric

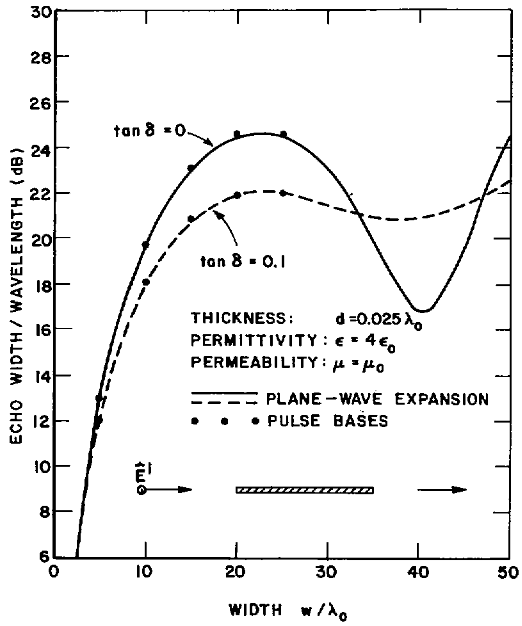

Fig. 5. Forward scatter versus width for thin dielectric strip with grazing incidence.

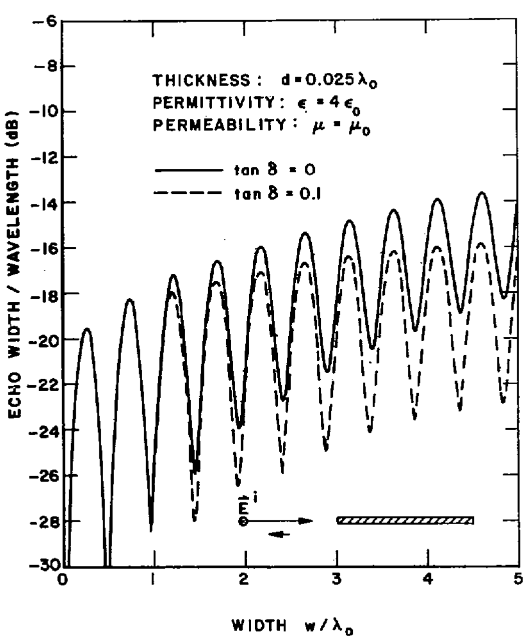

Fig. 6. Backscatter versus width for thin dielectric strip with grazing incidence, calculated with pulse basis.

field vector is parallel with the edges of the strip. The field in the dielectric region is expanded as the sum of three plane waves (the forced wave and two surface waves). The propagation constants are known for each wave, and Galerkin's method is employed to determine the amplitudes of these waves. Finally, the far-zone scattered field is determined by considering the polarization currents radiating in free space.

Numerical data are presented to illustrate the scattering properties of lossless and lossy dielectric strips as a function of the angle of incidence and the width of the strip. The calculations show excellent agreement with an earlier moment method using pulse bases and point matching.

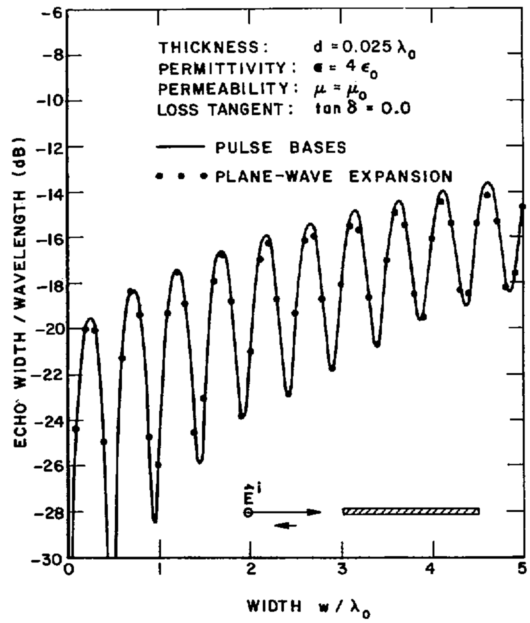

Fig. 7. Backscatter versus width for thin dielectric strip with grazing incidence.

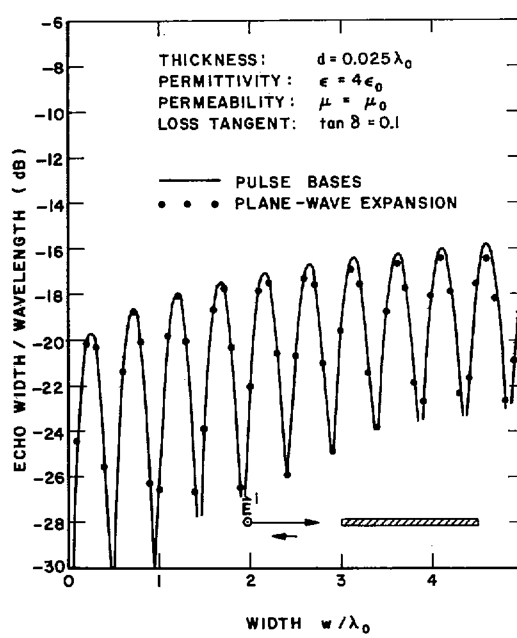

Fig. 8. Backscatter versus width for thin dielectric strip with grazing incidence.

APPENDIX
SURFACE WAVES

Let us consider a z-polarized surface wave propagating in the x direction on the lossy dielectric slab shown in Fig. 2. Let E^{I} denote the electric field intensity in region I (the dielectric slab) where the medium has parameters μ_1 and ϵ_1. Similarly, E^{II} denotes the electric field intensity in region II (outside the slab) where the ambient medium has parameters μ_2 and ϵ_2. For the mode that can propagate even on a very thin slab, the electric field intensity is given by

$$E_z^{\mathrm{I}} = B \exp(-fx) \cosh(g_1 y) \tag{36}$$

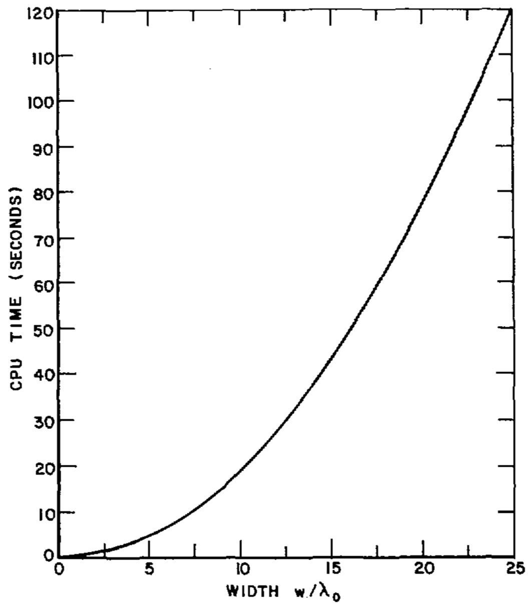

Fig. 9. Computer time versus width for thin dielectric strip with pulse bases.

$$E_z^{II} = A \exp(-fx) \exp(-g_2 y). \tag{37}$$

The magnetic field intensity has x and y components, and the x component is given by

$$H_x^{I} = -g_1 B \exp(-fx) \sinh(g_1 y)/(j\omega\mu_1) \tag{38}$$

$$H_x^{II} = g_2 A \exp(-fx) \exp(-g_2 y)/(j\omega\mu_2). \tag{39}$$

Enforcing continuity of E_z and H_x across the boundary at $y = t$, we find that

$$A \exp(-g_2 t) = B \cosh(g_1 t) \tag{40}$$

$$\mu_1 g_2 A \exp(-g_2 t) = -\mu_2 g_1 B \sinh(g_1 t). \tag{41}$$

From (40) and (41),

$$P = g_1 \tanh(g_1 t) + \mu_r g_2 = 0 \tag{42}$$

where $\mu_r = \mu_1/\mu_2$. From the wave equation,

$$g_1^2 = -\omega^2 \mu_1 \epsilon_1 - f^2 \tag{43}$$

$$g_2^2 = -\omega^2 \mu_2 \epsilon_2 - f^2. \tag{44}$$

We may use (43) and (44) to eliminate g_1 and g_2 in (42), so that P is a function of f. Letting P' denote the derivative of P with respect to f, we find that

$$P' = -[g_1 g_2 t \operatorname{sech}^2(g_1 t) + g_2 \tanh(g_1 t) + \mu_r g_1] f/(g_1 g_2). \tag{45}$$

For the surface wave, the complex x-axis propagation constant can be written as

$$f = \alpha + j\beta \tag{46}$$

where α and β are real. Let c denote the velocity of light in free space, and let v denote the phase velocity of the surface wave. Then

$$\beta = \omega\sqrt{\mu_0 \epsilon_0}\, c/v. \tag{47}$$

The Newton-Raphson method is most convenient for seeking a root of P in (42), and thus determining the propagation constant f.

REFERENCES

[1] J. H. Richmond, "Scattering by a dielectric cylinder of arbitrary cross section shape," *IEEE Trans. Antennas Propagat.*, vol. AP-13, pp. 334-341, May 1965.

[2] W. D. Burnside and K. W. Burgener, "High frequency scattering by a thin lossless dielectric slab," *IEEE Trans. Antennas Propagat.*, vol. AP-31, pp. 104-110, Jan. 1983.

[3] R. Kastner and R. Mittra, "A spectral-iteration technique for analyzing scattering from arbitrary bodies, part I: Cylindrical scatterers with E-wave incidence," *IEEE Trans. Antennas Propagat.*, vol. AP-31, pp. 499-506, May 1983.

[4] P. H. Pathak and R. Rojas-Teran, private communication, July 1983.

[5] R. F. Harrington, *Field Computation by Moment Methods.* New York: Macmillan, 1968.

[6] M. Abramowitz and I. A. Stegun, *Handbook of Mathematical Functions.* Washington, D.C.: National Bureau of Standards, 1964.

Jack H. Richmond (S'49-M'56-SM'59-F'80), for a photograph and biography please see page 182 of the March 1982 issue of this TRANSACTIONS.